JOURNAL OF PROPULSION AND POWER
Vol. 21, No. 5, September–October 2005

Discharge Current Oscillation in Hall Thrusters

Naoji Yamamoto*
Kyushu University, Fukuoka 816-8580, Japan
and
Kimiya Komurasaki† and Yoshihiro Arakawa‡
University of Tokyo, Tokyo 113-8656, Japan

The discharge current oscillation at a frequency range of 10–100 kHz in Hall thrusters was investigated with the objective of extending their stable operational range. The amplitude of oscillation was measured using two types of Hall thrusters—the anode layer type and the magnetic layer type. The oscillation amplitude was found to be sensitive to the applied magnetic flux density, and this result indicated that the oscillation was affected by electron mobility. An oscillation model was proposed based on the experimental results, and the predicted frequency and stable operational range were found to agree qualitatively agreed with the experimental results. This model shows that the momentum transfer corresponding to plasma fluctuation, that is, the viscosity effect, is crucial to achieving stability. Thus, the oscillation amplitude for various acceleration channel configurations—divergent, parallel, and convergent—was measured because the momentum transfer could be affected by the channel configuration. The stable operational range was successfully extended by the adoption of the convergent configuration in each type of Hall thruster, as shown by this model.

Nomenclature

B = magnetic flux density
D = diffusion coefficient
E = electric field strength
e = electronic charge
I = current
I_c = coil current
I_{sp} = specific impulse
k = wave number
k_B = Boltzmann's constant
L = ionization zone length
m = particle mass
$\dot{m}$ = mass flow rate
N = number density
r_L = Larmor radius
S = cross section
T = temperature
V = volume
V_e = electron velocity
V_n = neutral atom velocity
V_d = discharge voltage
z = axial direction
Δ = oscillation amplitude
η_a = acceleration efficiency
η_E = beam energy efficiency
λ_{ne} = neutral-electron mean free path
μ = mobility
σ_{di} = atom ionization collision cross section
σ_T = atom total collision cross section
τ = measurement time
ϕ = diameter
ω = oscillation frequency

Subscripts

a = anomalous diffusion
c = classical diffusion
d = discharge
e = electron
eff = effective
i = ion
n = neutral atom
out = outer
r = radial direction
0 = anode side
1 = exit side

Presented as Paper 2004-4100 at the AIAA/ASME/SAE/ASEE 40th Joint Propulsion Conference and Exhibit, Fort Lauderdale, FL, 11–14 July 2004; received 10 August 2004; revision received 30 March 2005; accepted for publication 3 March 2005.

*Research Associate, Department of Advanced Energy Engineering Science, Graduate School of Engineering Sciences, 6-1 Kasuga-kouen, Kasuga; yamamoto@aees.kyushu-u.ac.jp. Member AIAA.

†Associate Professor, Department of Aeronautics and Astronautics, Faculty of Engineering, Hongo 7-3-1, Bunkyo-ku. Member AIAA.

‡Professor, Department of Aeronautics and Astronautics, Faculty of Engineering, Hongo 7-3-1, Bunkyo-ku. Member AIAA.

Introduction

HALL thrusters show considerable promise for satellite station-keeping and orbit-transfer applications[1,2] because they offer an attractive combination of high thrust efficiency, exceeding 50%, with a specific impulse range of 1000–3000 s and a higher ion beam density than ion thrusters because of the existence of electrons in the ion acceleration zone. This is because a moderate magnetic field is applied in the acceleration zone, causing the magnetization of the electrons and not the ions.[3]

Several types of Hall thrusters are available, but they can be categorized into two general groups: the magnetic layer type and the anode layer type.[4,5] One example of the former type is the Russian stationary plasma thruster.[3,6] The distinguishing features of this type are continuous and extended acceleration zones for sufficient ionization and stability. It has a ceramic wall, and its acceleration channel length is longer than its channel width.[3] On the other hand, the thruster with anode layer, which was also developed in Russia,[7,8] is an example of the anode layer type. This thruster has a narrow acceleration zone for reducing the loss of ion and electron collisions with the walls.[9,10] It has a conducting wall, which potential is kept in a cathode potential and its acceleration channel length is shorter than its channel width. The electron temperature of this type of thruster is higher than that of the former because of the low electron energy losses to the wall.[5]

One of the challenges presented by Hall thrusters is the discharge current oscillation, particularly at a frequency range of 10–100 kHz

(Refs. 11 and 12). Because of the reduction in the impact of the power processing unit and the enlargement of the margin for the power supply of the satellite system, it is preferable to maintain a low level of discharge current oscillations. The oscillation may also affect the erosion of the acceleration channel or the ion beam divergence. Understanding the oscillation is essential for the future improvement of Hall thrusters, particularly of the anode layer type. Several studies have been conducted on this oscillation phenomenon, and they have revealed that the oscillation is caused by ionization instability.[13–17] However, these studies did not adequately describe the oscillation, and in particular, did not determine the stability criteria for a given range of magnetic flux density. The aim of the present study is 1) to propose a physical model related to the oscillation, 2) to validate the model by comparing the analytical and experimental results, and 3) to extend the stable operational condition range.

Experimental Equipment

Thruster

Figure 1a shows the cross section of a 1-kW class, anode-layer-type Hall thruster. The inner and outer diameters of the acceleration channel are 48 and 72 mm, respectively. The outer diameter can be changed to 62 mm. A solenoidal coil is set at the center of the thruster to apply a radial magnetic field in the acceleration channel. The magnetic flux density is varied by changing the coil current. There is no outer coil because a uniform magnetic field distribution is maintained along the azimuthal direction. The magnetic field distribution along the channel median is almost uniform in the short acceleration channel, as shown in Fig. 2. Magnetic flux density is maximized in the inner wall and decreases with an increase in radius because the magnetic flux is constant. Thus, in this study the magnetic flux density at the channel median is assumed to be representative. The guard rings are made of stainless steel (SUS304). The separation between the guard ring and the anode is 1 mm. It has a hollow annular anode, which comprises two cylindrical rings, and a propellant gas is fed through them. The position and the width of the hollow anode are varied by changing the anode components. In this study, the width of the hollow anode is 3 mm, and the gap between the tip of the anode and the exit of the acceleration channel is fixed at 8 mm ($\Phi_{out} = 72$ mm).

Figure 1b shows that a magnetic-layer-type Hall thruster can be achieved using an acceleration channel wall made of BN. The inner and outer diameters of the acceleration channel are 48 and 62 mm, respectively. The anode is located at 21 mm, upstream end of the acceleration channel.

Xenon gas was used as the propellant. A fresh filament cathode ($\phi = 0.27 \times 400$ mm $\times$ 3, 2% thoriated tungsten) was used as the electron source, because an old hollow cathode can be a noise source.[18] The thrust was measured using a pendulum-type thrust stand.[19] The error of the thrust measurement was below 2 mN. An ion-beam current was measured using the ion-beam collector (500×500 mm nude plane collector) that was located at 250 mm downstream of the thruster. Compensation for the decay of the ion beam current by charge-exchange was performed according to the method described in Ref. 20. The charge-exchange cross section was obtained from Ref. 21. The friction of the double xenon ion was assumed to be 0.2 (Refs. 22 and 23). The total error of this compensation did not exceed 5%, and the largest source of error is the ionization gauge.

Vacuum Chamber

A vacuum chamber of 2 m diameter by 3 m length was used in the experiments. The pumping system comprised a diffusion pump, a mechanical booster pump, and two rotary pumps. The background pressure was maintained below 5.3×10^{-3} Pa for most of the operating conditions.

Results and Discussion

Oscillation Characteristics

The amplitude of the discharge current oscillation should be a good indicator of stability because increasing oscillation could cause failure of the thruster. To evaluate the oscillation depth in the experimental results, the amplitude of oscillation Δ is defined as

$$\Delta = \frac{\text{R.M.S}}{\overline{I_d}} = \frac{1}{\overline{I_d}}\sqrt{\frac{\int_0^\tau (I_d - \overline{I_d})^2\,\mathrm{d}t}{\tau}}, \qquad \left(\overline{I_d} = \frac{\int_0^\tau I_d\,\mathrm{d}t}{\tau}\right) \tag{1}$$

Figure 3 shows the relation between thrust performance and magnetic flux density. The oscillation amplitude sensitively changed with B. Stable operation was observed in a very narrow range near

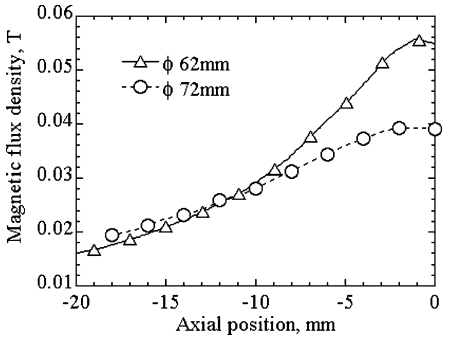

a)

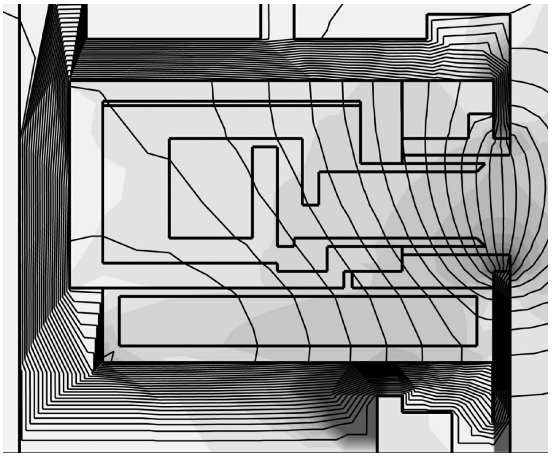

b)

Fig. 2 Magnetic field configuration of the Hall thruster developed at the University of Tokyo: a) radial magnetic flux density profile and b) calculated magnetic field lines ($\phi_{out} = 72$ mm) (calculated using Students' QuickField 3.4, Tera Analysis Company).

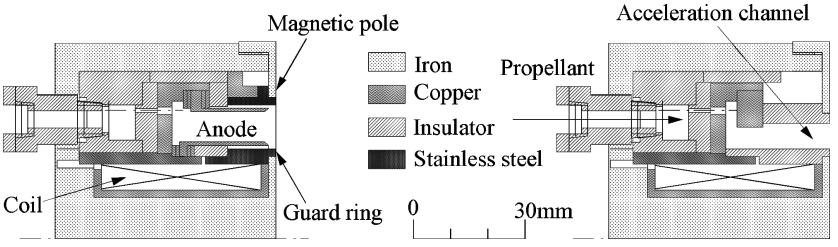

a) b)

Fig. 1 Cross section of the Hall thruster developed at the University of Tokyo: a) anode layer type and b) magnetic layer type.

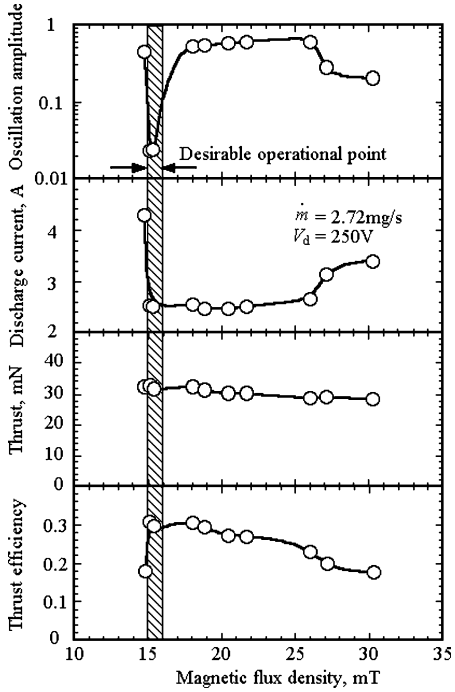

Fig. 3 Oscillation characteristics: anode layer type, $\phi_{out} = 72$ mm, $\dot{m} = 2.72$ mg/s, and $V_d = 250$ V.

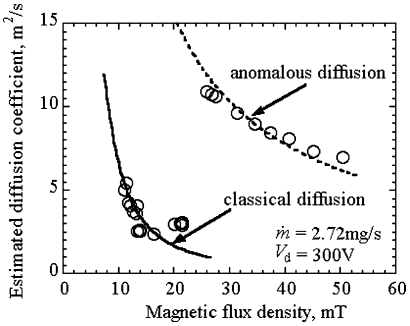

Fig. 4 Estimated electron diffusion coefficient: anode layer type, $\phi_{out} = 72$ mm, $\dot{m} = 2.72$ mg/s, and $V_d = 300$ V.

$B \approx 16$ mT or $B > 27$ mT in this configuration, although the thrust efficiency was low for $B > 27$ mT. This is because the discharge current suddenly increases at $B = 27$ mT. Thus, the operational condition range was narrow, and hence an extension of the stable operational condition range is required. This sensitivity to B indicates that the oscillation would be dominated by electron mobility rather than by ion mobility.

The transition in operational regime at $B = 27$ mT is caused by the transition in electron diffusion from classical to anomalous diffusion. That is, an electron moves toward the anode via classical diffusion when $B < 27$ mT, and it moves via anomalous diffusion when $B > 27$ mT, as shown in Fig. 4. The diffusion coefficient at the acceleration channel exit was estimated as follows:

$$D = \frac{\Gamma_e}{S\,N_e[(e/kT_e)E + \nabla n_e/N_e]} \Rightarrow D_1 \approx \frac{I_d - I_i}{eS_1 N_{i1}(e/kT_{e1})E_1} \quad (2)$$

I_i was measured by the ion collector and the number density of ions was estimated as follows:

$$N_{i1} = I_i/eS_1V_{i1} \approx I_i \Big/ eS_1\sqrt{2\eta_E eV_d/m_i} \quad (3)$$

The values of beam energy efficiency[24] E, and T_e were assumed to be typical measurement values, as shown in Table 1, where η_E was measured by means of a retarding potential analyzer,[25] and T_e was measured by means of a double Langmuir probe.[26] E was estimated to be 1.2 (300 V/250 V) times that of the results measured by means of an emissive probe.[27] I_i was measured by means of the ion collector. The oscillation regime also changes at this point. This was another indication that the oscillation is sensitive to electron mobility.

Table 1 Typical measurement values for estimation of diffusion coefficient

Parameter	Classical diffusion regime	Anomalous diffusion regime
η_E	0.9	0.8
T_e, eV	16	12
E, V/m	60,000	24,000

Oscillation Model

Several studies have indicated that the discharge current oscillation is caused by the so-called "breathing mode" ionization instability,[13–17] that is, the disturbance in the number density of neutral atoms causes the disturbance in plasma density, and it feeds back to the disturbance of neutral atom density. There is a time lag between the neutral atom feed and the plasma feed, so that the number density in each particle continues oscillating without convergence. Baranov's model[13,14] does not adequately describe this oscillation, however, particularly with respect to the stability criteria for a certain range of magnetic flux density. Thus, a revised ionization instability model was proposed.

The set of equations describing this oscillation is as follows: the equation of continuity for the neutral atom and the equation of continuity for the electron. The continuity for the ion was not adopted[15] because the diffusion rate of plasma is controlled by the slower species, which is the electron in the Hall thrusters, where the electron is trapped by the magnetic field.

The equation of continuity for the neutral atom is written as follows:

$$\int_V \frac{\partial N_n}{\partial t}\,\mathrm{d}V + \int_S N_n V_n\,\mathrm{d}S = \int_V -\langle\sigma_{\mathrm{di}} v_e\rangle_{T_e} N_n N_e\,\mathrm{d}V \quad (4)$$

The equation of continuity for the electron is written as follows:

$$\int_V \frac{\partial N_e}{\partial t}\,\mathrm{d}V + \int_S N_e V_e\,\mathrm{d}S = \int_V \langle\sigma_{\mathrm{di}} v_e\rangle_{T_e} N_n N_e\,\mathrm{d}V \quad (5)$$

Linearization was performed to solve these equations analytically. The phase velocity of perturbation of neutral atoms was propagated as its axial velocity. The tide of the neutral atom density was compensated by the movement of the neutral particle; thus, we assume that the perturbation was propagated with the axial velocity of the neutral particle atom. In the Hall-thruster acceleration channel, the neutral atom axial velocity is assumed to be

$$V_n = \frac{1}{2}\sqrt{\frac{2k_bT_n}{\pi m_n}} = 100 \text{ m/s} \quad (6)$$

because the temperature of the neutral particles is estimated to be 1000 K (Ref. 28). On the other hand, the wave number of plasma was assumed to be zero because plasma in the ionization zone will fluctuate monolithically.[29] This is a unique feature of this model and is acceptable because the relaxation time of plasma $[\approx (L/\pi)^2/2D_e \approx (3 \times 10^{-3}/\pi)^2/(2 \times 3) \approx 0.2\ \mu\mathrm{s}]$ is less than the oscillation period ($\approx 30\ \mu$s), although Baranov assumed that perturbation of plasma would be propagated with the same phase velocity as the disturbance of the neutral atoms.[14] The imaginary part of k_n, which is the decay term, was assumed to be equal to $1/\lambda_{\mathrm{ne}}$ because the number density of the neutral atom in the acceleration channel would decay by ionization.

$$N_n = N_n + n_n \exp[-i(\omega t - k_n z)] \quad (7)$$

$$N_e = N_e + n_e \exp[-i\omega t] \quad (8)$$

where $k_n = C_n + i\,1/\lambda_{\mathrm{ne}}$, and $C_n \approx \mathrm{Re}[\omega]/2\pi V_n$.

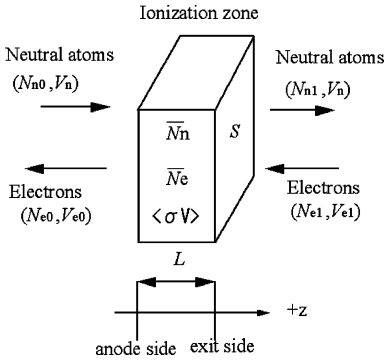

Fig. 5 Schematic representation of the ionization zone in the present model.

For simplicity, $\langle \sigma_{\mathrm{di}} v_e \rangle_{T_e}$, N_n, N_e is considered as $\overline{\langle \sigma_{\mathrm{di}} v_e \rangle_{T_e}}$, $\bar{N}_n$, $\bar{N}_e$ and the boundary condition are defined as shown in Fig. 5:

$$\overline{\langle \sigma_{\mathrm{di}} v_e \rangle_{T_e}} = \frac{1}{L}\int_0^L \langle \sigma_{\mathrm{di}} v_e \rangle_{T_e}\,\mathrm{d}z$$

$$\bar{N}_n = \frac{1}{L}\int_0^L N_n\,\mathrm{d}z, \qquad \bar{N}_e = \frac{1}{L}\int_0^L N_e\,\mathrm{d}z \tag{9}$$

If the electron moves to the anode with classical diffusion, the electron velocity is assumed to oscillate. This is because the electron velocity is proportional to the neutral atom density. The electron velocity is written as follows:

$$V_e = V_e + v_e = -\frac{m_e \langle \sigma_T v_e \rangle_{\mathrm{en}}}{eB^2}\left(E + \frac{k_B T_e}{e}\frac{\nabla N_e}{N_e}\right)(N_n + n_n)$$

$$\equiv f(z)(N_n + n_n) \tag{10}$$

Substituting Eqs. (7) and (8) into Eqs. (4) and (5), the dispersion relation is written as

$$\omega^2 + \left\{ i\overline{\langle \sigma_{\mathrm{di}} v_e \rangle}_{T_e}(\bar{N}_e - \bar{N}_n) + i[(V_{e1} - r_S V_{e0})/L] - GV_n \right\}\omega + iG\left(\overline{\langle \sigma_{\mathrm{di}} v_e \rangle}_{T_e}\bar{N}_n V_n - [(V_{e1} - r_S V_{e0})/L]V_n + \overline{\langle \sigma_{\mathrm{di}} v_e \rangle}_{T_e}\bar{N}_n f_1 N_{e1}\right) - \overline{\langle \sigma_{\mathrm{di}} v_e \rangle}_{T_e}\bar{N}_e[(V_{e1} - r_S V_{e0})/L] = 0 \tag{11}$$

where

$$G = \frac{k_n \times \exp[ik_n L]}{\exp[ik_n L] - 1}$$

and $r_S = S_0/S_1$.

After solving the preceding dispersion relation, the frequency of this oscillation $\mathrm{Re}[\omega]$ is written as follows:

$$f_c = (1/2\pi)\mathrm{Re}[\omega]$$

$$= (1/2\pi)\left\{\tfrac{1}{2}(-a_c + \mathrm{Re})\left[\sqrt{(a_c + ib_c)^2 - 4(c_c + id_c)}\right]\right\} \tag{12}$$

The stability condition of this oscillation $\mathrm{Im}[\omega] < 0$ is written as follows:

$$b_c > 0 \tag{13}$$

$$b_c^2 c_c - a_c b_c d_c + d_c^2 < 0 \tag{14}$$

where

$$a_c = -\mathrm{Re}[G] \times V_n$$

$$b_c = (V_{e1} - r_S V_{e0})/L - \overline{\langle \sigma_{\mathrm{di}} v_e \rangle}_{T_e}\bar{N}_n + \overline{\langle \sigma_{\mathrm{di}} v_e \rangle}_{T_e}\bar{N}_e - \mathrm{Im}[G] \times V_n$$

$$c_c = -\mathrm{Im}[G] \times \left(\overline{\langle \sigma_{\mathrm{di}} v_e \rangle}_{T_e}\bar{N}_n V_n - [(V_{e1} - r_S V_{e0})/L]V_n + \overline{\langle \sigma_{\mathrm{di}} v_e \rangle}_{T_e}N_n f_1 N_{e1}\right) - \overline{\langle \sigma_{\mathrm{di}} v_e \rangle}_{T_e}\bar{N}_e[(V_{e1} - r_S V_{e0})/L]$$

$$d_c = \mathrm{Re}[G] \times \left(\overline{\langle \sigma_{\mathrm{di}} v_e \rangle}_{T_e}\bar{N}_n V_n - [(V_{e1} - r_S V_{e0})/L]V_n + \overline{\langle \sigma_{\mathrm{di}} v_e \rangle}_{T_e}N_n f_1 N_{e1}\right)$$

If the electron moves to the anode according to anomalous diffusion, under which the diffusion coefficient does not depend on the neutral atom number density, the electron velocity is written as follows:

$$V_e = -\mu E - D(\nabla n_e/n_e) = -\mu_{\mathrm{eff}}[E + (kT_e/e)(\nabla n_e/n_e)] \tag{15}$$

Thus, the dispersion relation is written as follows:

$$\omega^2 + \left\{-i\overline{\langle \sigma_{\mathrm{di}} v_e \rangle}_{T_e}\bar{N}_n + i[(V_{e1} - r_S V_{e0})/L] + i\overline{\langle \sigma_{\mathrm{di}} v_e \rangle}_{T_e}\bar{N}_e - GV_n\right\}\omega + iGV_n\left(\overline{\langle \sigma_{\mathrm{di}} v_e \rangle}_{T_e}\bar{N}_n - (V_{e0} - r_S V_{e1})/L\right) - \overline{\langle \sigma_{\mathrm{di}} v_e \rangle}_{T_e}\bar{N}_e[(V_{e1} - r_S V_{e0})/L] = 0 \tag{16}$$

The frequency of this oscillation $\mathrm{Re}[\omega]$ is written as follows:

$$f_a = (1/2\pi)\mathrm{Re}[\omega]$$

$$= (1/2\pi)\left(\tfrac{1}{2}\left\{-a_a + \mathrm{Re}\left[\sqrt{(a_a + ib_a)^2 - 4(c_a + id_a)}\right]\right\}\right) \tag{17}$$

The stability condition of this oscillation $\mathrm{Im}[\omega] < 0$ is written as follows:

$$b_a > 0 \tag{18}$$

$$b_a^2 c_a - a_a b_a d_a + d_a^2 < 0 \tag{19}$$

where

$$a_a = -\mathrm{Re}[G] \times V_n$$

$$b_a = (V_{e1} - r_S V_{e0})/L - \overline{\langle \sigma_{\mathrm{di}} v_e \rangle}_{T_e}\bar{N}_n + \overline{\langle \sigma_{\mathrm{di}} v_e \rangle}_{T_e}\bar{N}_e - \mathrm{Im}[G] \times V_n$$

$$c_a = -\mathrm{Im}[G] \times \left(\overline{\langle \sigma_{\mathrm{di}} v_e \rangle}_{T_e}\bar{N}_n V_n - [(V_{e1} - r_S V_{e0})/L]V_n\right) - \overline{\langle \sigma_{\mathrm{di}} v_e \rangle}_{T_e}\bar{N}_e[(V_{e1} - r_S V_{e0})/L]$$

$$d_a = \mathrm{Re}[G] \times \left(\overline{\langle \sigma_{\mathrm{di}} v_e \rangle}_{T_e}\bar{N}_n V_n - [(V_{e1} - r_S V_{e0})/L]V_n\right)$$

Figure 6 shows the measured and predicted oscillation frequencies. In the anode-layer-type thruster, the predicted frequency was obtained from Eq. (12) because the electron moves to the anode with classical diffusion. For both the experiment and the calculation, $\phi_{\mathrm{out}} = 72$ mm, $\dot{m} = 2.04$ mg/s, and $B_r = 16$ mT. On the other hand, in the magnetic-layer-type thruster, the predicted frequency was obtained from Eq. (17) because of the presence of anomalous conductivity.[4] For both the experiment and the calculation, $\dot{m} = 1.36$ mg/s and $B_r = 14$ mT. The effective electron mobility was assumed to be the Bohm mobility,[30] $1/16B$. This might be an oversimplification, but it should be adequate to observe the qualitative characteristics of the oscillation. It is more appropriate to

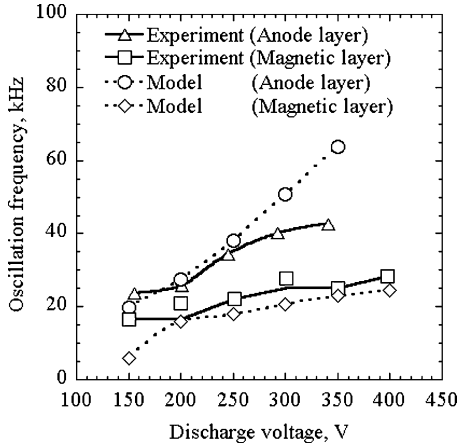

Fig. 6 Relation between the oscillation frequency and discharge voltage: anode layer type, $\phi_{\mathrm{out}} = 72$ mm, $\dot{m} = 2.04$ mg/s, and $B_r = 16$ mT; and magnetic layer type, $\dot{m} = 1.36$ mg/s, and $B_r = 14$ mT.

consider the anomalous diffusion because of circumferential plasma fluctuation[31] or the so-called near-wall conductivity.[32] That is, the term that is proportional to the square of the perturbation of number density should be added to the mobility in classical diffusion.[9,31] Alternatively, the effective collision cross section or the assumed effective mobility coefficient $1/\alpha B$ (Ref. 33), where α is a fitting parameter that does not depend on the electron energy, could be used. However, the unresolved subject of electron transport in Hall thrusters is debatable.[33–35] This oscillation model might become extremely complex and questionable if the anomalous diffusion caused by the previously-mentioned physical phenomena is considered. In addition, there is no warrant that the value of the effective diffusion coefficient, α, was assumed as particular value.

The oscillation frequency calculated using this model agreed qualitatively with the measured frequency. That is, both increased with an increase in discharge voltage. This tendency can be explained as follows. To simplify Eqs. (12) or (17), the oscillation frequency can be rewritten as follows:

$$f \approx \sqrt{\langle \sigma_{\mathrm{di}} v_e \rangle_{T_e} \bar{N}_e [(V_{e1} - r_S V_{e0})/L]} \tag{20}$$

This equation indicates that the oscillation frequency increases with an increase in electron temperature. Thus, oscillation frequency would increase with an increase in the discharge voltage because electron temperature would increase with an increase in the discharge voltage. This also indicates why the frequency of the anode-layer-type thruster was higher than that of the magnetic layer type; the electron temperature of the anode-layer-type thruster will be higher than that of the magnetic layer type,[5] as indicated by the experimental results.

Figures 7 and 8 show the measured oscillation amplitude and the predicted range of stable operational conditions. The hatched area indicates predicted stable operational conditions deduced from the present model, and the doted area indicates the same as deduced from Baranov's model.[14] The blank area indicates the unavailability of data for those conditions. Experimental results have shown that

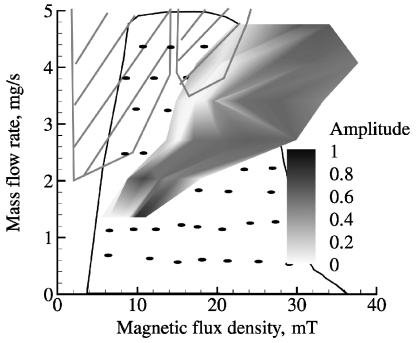

Fig. 7 Map of stable/unstable operation conditions: anode layer type, $V_d = 250$ V.

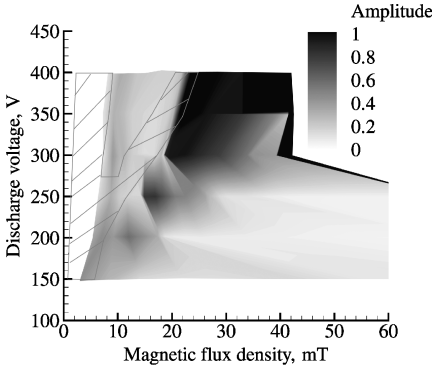

Fig. 8 Map of stable/unstable operation conditions: magnetic layer type, $\dot{m} = 1.36$ mg/s.

the stable operational range of B was increased with an increase in $\dot{m}$. In addition, there were stable operations with low magnetic flux density, although η_a was low.[18,24] With an increase in B, operational conditions changed from stable to unstable and back to stable, and then to unstable again.

The stable condition according to the Baranov's model is written as follows:

$$\left(\frac{\partial D_e}{\partial x} - V_n\right)^2 > \frac{(N_n - N_e)^2}{N_n} D_e \langle \sigma_{\mathrm{di}} v_e \rangle_{T_e} \tag{21}$$

Equation (21), however, can be rewritten as $\dot{m} < \text{const}$—B^{-3} and $\dot{m} < B^{-3}$ and $V_d < B^{\alpha}(1 < \alpha < 1.5)$ and $V_d < B^{-3}$ (see Ref. 14). That is, the stable operational range of B decreases with an increase in $\dot{m}$. In addition, Baranov's model cannot predict the stable operation at the low magnetic flux density. Thus, it will not adequately describe the present oscillation.

On the other hand, the predicted stable operational condition range deduced from the present model qualitatively agreed with the experimental results. That is, the predicted stable operational range of B would increase with an increase in $\dot{m}$. It also predicts that with an increase in B, the operational condition would be changed from stable to unstable and back to stable and unstable again. Hence, the present model would provide a good explanation of the oscillation mechanism, and the validity of the model would be proven. The model can be simplified, and the conditions of stable operations rewritten as follows:

$$S_1 V_{e1} - S_0 V_{e0} - (\sigma_{\mathrm{di}} v_e)_{T_e} > 0 \tag{22}$$

The left-hand side of Eq. (22) represents the momentum transfer corresponding to fluctuations of plasma, that is, viscosity effects. Thus, the oscillations decay if the viscosity coefficient, that is, the left-hand side of Eq. (22), is positive.

In addition, this model shows why the stable operation of the anode layer is narrower than that of the magnetic layer:

1) Electrons move to the anode with classical diffusion in the anode-layer-type configuration. Thus, as shown in Eq. (22), stable operation is more sensitive to B in the anode layer type than in the magnetic layer type.

2) The electron temperature of the anode-layer-type configuration will be higher than that of the magnetic layer type. Thus, the left-hand side of Eq. (22) can more easily become negative in the anode layer type than in the magnetic layer type.

Reduction of the Oscillation Amplitude

Equation (22) shows that an increase in $S_0 V_{e0}/S_1 V_{e1}$ will make the operation stable. Thus, the oscillation amplitude was measured for various guard rings, as shown in Fig. 9, because the channel configuration would affect the propellant utilization, resulting in a change in V_{e1} under classical diffusion. The inner and outer diameters of the guard rings of the divergent type are 46 and 64 mm, respectively. The outer diameter of the convergent type is 60 mm. The present model predicts that the stable operational condition range of the convergent type is the widest, and that of the divergent type is the narrowest among the three configurations that were considered. Figure 10 shows the measured oscillation amplitude for the various guard rings. The stable operational range was successfully extended with the adoption of the convergent configuration, as shown by this

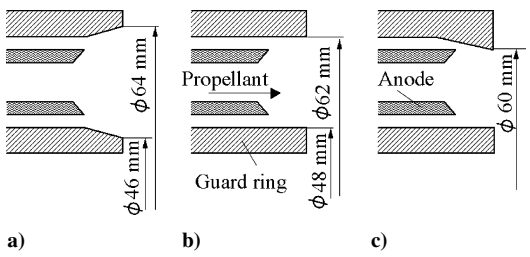

Fig. 9 Various guard rings, anode-layer-type configuration: a) divergent, b) parallel, and c) convergent.

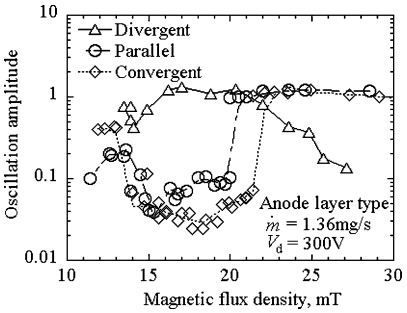

Fig. 10 Oscillation amplitude for various guard rings: anode layer type, $\phi_{out} = 62$ mm, $\dot{m} = 1.36$ mg/s, and $V_d = 300$ V.

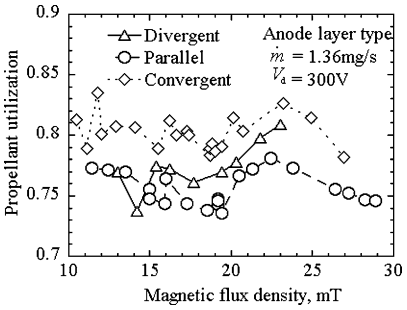

Fig. 11 Propellant utilization for various guard rings: anode layer type, $\phi_{out} = 62$ mm, $\dot{m} = 1.36$ mg/s, and $V_d = 300$ V.

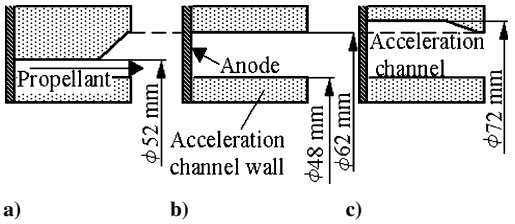

Fig. 12 Various acceleration channels, magnetic-layer-type configuration: a) divergent, b) parallel, and c) convergent.

model. In addition, the propellant utilization of the convergent type was the largest among the three, as shown in Fig. 11, and the thrust efficiency of the convergent type was obviously the best. Because the magnetic flux density at the transition from classical diffusion to anomalous diffusion in the anode layer/divergent configuration is lower than that in the others, the oscillation amplitude in the divergent configuration is small when the magnetic flux density is greater than 22 mT. Under the anomalous diffusion condition, the relation of oscillation characteristics to the magnetic flux density was almost the same as that under the classical diffusion, as shown in Figs. 3 and 4.

This model also shows that in a magnetic-layer-type configuration the adoption of a convergent acceleration channel would extend the range of stable operation conditions because S_0/S_1 can be increased while maintaining the value of V_{e0}/V_{e1}. Hence, the oscillation amplitude was measured for various acceleration channel configurations, as shown in Fig. 12. The inner and outer diameters of the divergent type of acceleration channel are 48 and 52 mm, respectively. The outer diameter of the convergent type is 72 mm. The divergent type cannot maintain the discharge for $\dot{m} = 1.36$–2.72 mg/s, $V_d = 150$–400 V, and $B_r = 0$–0.06 T. Figure 13 shows the operational condition map with the convergent acceleration channels. The stable operational condition range of convergent type is larger than that of the parallel type as shown in Fig. 8. Thus, the stable operational condition range for both the anode layer type and the magnetic layer type thrusters was successfully extended.

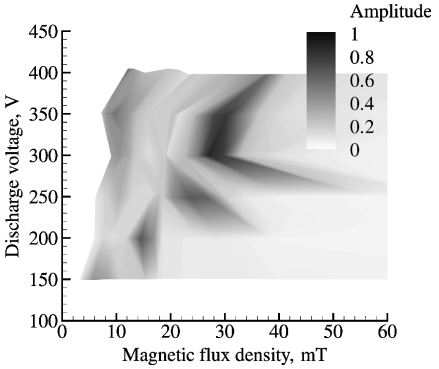

Fig. 13 Map of stable/unstable operation conditions with convergent acceleration channel: magnetic layer type, $\dot{m} = 1.36$ mg/s.

Conclusions

A discharge current oscillation at a frequency range of 10–100 kHz was investigated using a 1-kW-class Hall thruster. The oscillation amplitude was sensitive to the magnetic flux density, and the oscillation characteristics were changed when the transition from classical to anomalous electron diffusion occurred. These experimental results indicated that electron mobility affects this oscillation. Therefore, an oscillation model that took the electron dynamics into consideration was proposed. The predicted frequency and the stable operational condition range agreed qualitatively with the experimental results, and thus the validity of the model was proven. This model also showed that the difference in oscillation characteristics between the magnetic-layer-type and the anode-layer-type thrusters is caused by the difference in the electron diffusion form and the difference in the electron temperature. The present model also shows that acceleration channel configuration affects the oscillation. The convergent acceleration channel configuration leads to an increase in the viscosity of plasma; this allows the stable operational range to expand. On the other hand, the divergent channel configuration reduces the stable operational range. Thus, the stable operational range for various acceleration channel configurations was investigated, and the experimental results for each type of Hall thruster successfully validated this procedure.

Acknowledgment

The present work was supported by a Grant-in-Aid for Scientific Research (S), No. 16106012, sponsored by the Ministry of Education, Culture, Sports, Science and Technology, Japan.

References

[1]Saccoccia, G., "Introduction to the European Activities in Electric Propulsion," *Proceedings of the 28th International Electric Propulsion Conference*, IEPC, Paper 03-341, March 2003.

[2]Blandino, J., "The Year in Review, Electric Propulsion," *Aerospace America*, Dec. 2003, pp. 60, 61.

[3]Kim, V., "Main Physical Features and Processes Determining the Performance of Stationary Plasma Thrusters," *Journal of Propulsion and Power*, Vol. 14, No. 5, 1998, pp. 736–743.

[4]Kaufman, H. R., "Technology of Closed-Drift Thrusters," *AIAA Journal*, Vol. 23, No. 1, 1985, pp. 78–86.

[5]Choueiri, E. Y., "Fundamental Difference Between the Two Hall Thruster Variants," *Physics of Plasmas*, Vol. 8, No. 11, 2001, pp. 5025–5033.

[6]Morozov, A. I., Esipchuk, Yu. V., Tilinin, G. N., Trofimov, A. V., Sharov, Yu. A., and Shchepkin, G. Ya., "Plasma Accelerator with Closed Electron Drift and Extended Acceleration Zone," *Soviet Physics-Technical Physics*, Vol. 17, No. 1, 1972, pp. 38–45.

[7]Zharinov, A. V., and Popov, Yu. S., "Acceleration of Plasma by a Closed Hall Current," *Soviet Physics-Technical Physics*, Vol. 12, No. 2, 1967, pp. 208–211.

[8]Semenkin, A., "Investigation of Erosion in Anode Layer Thrusters and Elaboration High Life Design Scheme," *Proceedings of the 23rd International Electric Propulsion Conference*, IEPC, Paper 93-231, Electric Rocket Propulsion Society, Sept. 1993.

[9]Popov, Yu. S., and Zolotaikin, Yu. M., "Effect of Anomalous Conductivity on the Structure of the Anode Sheath in a Hall Current Ion Source," *Soviet Journal of Plasma Physics*, Vol. 3, No. 2, 1977, pp. 210–213.

[10]Zhurin, V. V., Kaufman, H. R., and Robinson, R. S., "Physics of Closed Drift Thrusters," *Plasma Sources Science and Technology*, Vol. 8, No. 1, 1999, pp. R1–R20.

[11]Tilinin, G. N., "High-Frequency Plasma Waves in a Hall Accelerator with an Extended Acceleration Zone," *Soviet Physics-Technical Physics*, Vol. 22, No. 8, 1977, pp. 974–978.

[12]Choueiri, E. Y., "Plasma Oscillations in Hall Thrusters," *Physics of Plasmas*, Vol. 8, No. 4, 2001, pp. 1411–1426.

[13]Baranov, V. I., Nazarenko, Yu. S., Petrosov, V. A., Vasin, A. I., and Yashonov, Yu. M., "Theory of Oscillations and Conductivity for Hall Thruster," AIAA Paper 96-3192, July 1996.

[14]Baranov, V. I., Nazarenko, Yu. S., Petrosov, V. A., Vasin, A. I., and Yashonov, Yu. M., "The Ionization Oscillations Mechanism in ACD," *Proceedings of the 24th International Electric Propulsion Conference*, IEPC, Paper 95-059, Sept. 1995.

[15]Fife, J. M., Martinez-Sanchez, M., and Szabo, J., "A Numerical Study of Low-Frequency Discharge Oscillations in Hall Thrusters," AIAA Paper 97-3052, July 1997.

[16]Boeuf, J. P., and Garrigues, L., "Low Frequency Oscillation in a Stationary Plasma Thruster," *Journal of Applied Physics*, Vol. 84, No. 7, 1998, pp. 3541–3554.

[17]Komurasaki, K., and Kusamoto, D., "Optical Measurement of Plasma Oscillations in a Hall Thruster," *Transactions of the Japan Society for Aeronautical and Space Sciences*, Vol. 42, No. 134, 1999, pp. 203–208.

[18]Yamamoto, N., Komurasaki, K., and Arakawa, Y., "Condition of Stable Operation in a Hall Thruster," *Proceedings of the 28th International Electric Propulsion Conference*, IEPC, Paper 03-086, March 2003.

[19]Sasoh, A., and Arakawa, Y., "A High Resolution Thrust Stand for Ground Tests of Low-Thrust Space Propulsion Devices," *Review of Scientific Instruments*, Vol. 64, No. 3, 1993, pp. 719–723.

[20]Rapped, D., and Francis, W. E., "Charge Exchange Between Gaseous Ions and Atoms," *Journal of Chemical Physics,* Vol. 37, No. 11, 1962, pp. 2631–2645.

[21]Sanborn, C. B., *Basic Data of Plasma Physics*, 1966, 2nd ed., MIT Press, Cambridge, MA, 1967, p. 75.

[22]Gallimore, A. D., "Near- and Far-Field Characterization of Stationary Plasma Thruster Plumes," *Journal of Spacecraft and Rockets*, Vol. 38, No. 3, 2001, pp. 441–453.

[23]Manzalla, D. H., and Sankovic, J. M., "Hall Thruster Ion Beam Characterization," AIAA Paper 95-2927, July 1995.

[24]Komurasaki, K., and Arakawa, Y., "Hall-Current Ion Thruster Performance," *Journal of Propulsion and Power*, Vol. 8, No. 6, 1992, pp. 1212–1216.

[25]Kakimoto, H., "Plasma Characteristics in Anode Layer Thrusters," M.S. Thesis, Dept. of Aeronautics and Astronautics, Univ. of Tokyo, March 2000 (in Japanese).

[26]Yamamoto, N., "Discharge Current Oscillation in Hall Thrusters," Ph.D. Dissertation, Dept. of Aeronautics and Astronautics, Univ. of Tokyo, March 2004 (in Japanese).

[27]Yamamoto, N., Nakagawa, T., Komurasaki, K., and Arakawa, Y., "Influence of Discharge Oscillation on Hall Thruster Perfomance," *Proceedings of the 27th International Electric Propulsion Conference*, IEPC, Paper 01-055, Electric Rocket Propulsion Society, Oct. 2001.

[28]Mazouffre, S., Pagnon, D., Lasgorceix, P., Touzeru, M., "Temperature of Xenon Atoms in a Stationary Plasma Thruster," IEPC, Paper 2003-283, March 2003.

[29]Yamamoto, N., Komurasaki, K., and Arakawa, Y., "Control of Discharge Current Oscillation in Hall Thrusters," *Proceedings of the 24th International Symposium on Space Technology and Science*, edited by J. Onodera, Japan Society for Aeronautical and Space Sciences and Organizing Committee of the ISTS, Tokyo, 2004, pp. 191–196.

[30]Bohm, D., "The Characteristics of Electrical Discharges in Magnetic Fields," *Qualitative Description of the Arc Plasma in a Magnetic Field*, edited by A. Guthrie and R. K. Wakenling, 1st ed., McGraw–Hill, New York, 1949, pp. 1–12.

[31]Yoshikawa, S., and Rose, J., "Anomalous Diffusion of a Plasma Across a Magnetic Field," *Physics of Fluids*, Vol. 5, No. 3, 1962, pp. 334–340.

[32]Bishaev, A. M., and Kim, V., "Local Plasma Properties in a Hall-Current Accelerator with an Extended Acceleration Zone," *Soviet Physics-Technical Physics*, Vol. 23, No. 9, 1978, pp. 1055–1057.

[33]Smirnov, A., Raitses, Y., and Fisch, N. J., "Electron Cross-Field Transport in a Low Power Cylindrical Hall Thruster," *Physics of Plasmas*, Vol. 11, No. 11, 2004, pp. 4922–4933.

[34]Hirakawa, M., and Arakawa, Y., "Numerical Simulation of Plasma Particle Behavior in a Hall Thruster," AIAA Paper 96-3195, July 1996.

[35]Meezan, N. B., Hargus, W. A., Jr., and Cappelli, M. A., "Anomalous Electron Mobility in a Coaxial Hall Discharge Plasma," *Physical Review E*, Vol. 63, No. 2, 026410, 2001.